The 5th International Symposium - Supercritical CO_2 Power Cycles
March 28-31, 2016, San Antonio, Texas

S-CO_2 cycle design and control strategy for the SFR application

Yoonhan Ahn
Korea Advanced Institute of Science and Technology
Department of Mechanical Engineering
Daejeon, South Korea

Min Seok Kim
Korea Advanced Institute of Science and Technology
Department of Nuclear and Quantum Engineering
Daejeon, South Korea

Jeong Ik Lee
Korea Advanced Institute of Science and Technology
Department of Nuclear and Quantum Engineering
Daejeon, South Korea

Yoonhan Ahn is a Ph.D candidate of Nuclear and Quantum Engineering department in KAIST. He has five years of experience in designing and modeling of various power conversion systems including supercritical carbon dioxide cycle for various applications.

Min Seok Kim is a Ph.D candidate of Nuclear and Quantum Engineering department in KAIST. He has two years of experience in designing and modeling of supercritical carbon dioxide cycle for various applications.

Jeong Ik Lee is an associate professor of Nuclear and Quantum Engineering department in KAIST. He has been leading the development of the supercritical carbon dioxide cycle in Korea.

Abstract

As a part of Sodium-cooled Fast Reactor development in Korea, the supercritical CO_2 Brayton cycle is studied as an alternative power conversion system to the steam Rankine cycle. The benefits of the S-CO_2 cycle are relatively high efficiency under the mild turbine inlet temperature condition, simple layout and compact size. In addition, the safety of the SFR system can be potentially enhanced as the violent sodium-water reaction can be replaced with the benign sodium-CO_2 reaction. The power output of the reference SFR is 150MWe, and two modules of 75MWe S-CO_2 recompression cycle will be used for the reference SFR application. The main components including turbomachineries and heat exchangers are designed with in-house codes which have been validated with experiment data. Based on the cycle and component design condition, the pipe system is designed and the component module arrangement and respective size are assessed. Due to the high mass flow rate and pressure drop in pipes, some portion of the cycle efficiency is reduced. To deal with the leakage flow from turbomachineries, the recovery system design condition is also assessed. Based on the designed components, the S-CO_2 cycle performance under part load condition is analyzed with an in-house developed quasi-static cycle analysis code. Furthermore, the control logics including inventory control, turbine bypass and throttle valve control are compared under the cycle part load performance.

I. Introduction

As the global climate change becomes substantial, an interest on the energy sources which have high efficiency and less CO_2 emission are increasing. The nuclear power is considered as one of the most promising candidates to attain the sustainability and economics at the same time. Currently, various countries are cooperating for the Gen IV reactor development to improve the system efficiency and safety of current conventional nuclear power system. Among the futuristic reactor designs, the Sodium-cooled Fast Reactor (SFR) researches are active in many countries due to abundant operating experiences in several leading countries. However, the violent sodium-water reaction has been a concern for winning the public acceptance.

The supercritical CO_2 cycle is considered as one of the potential alternatives that can replace the conventional steam Rankine cycle. The advantages of the S-CO_2 cycle are relatively high efficiency in the moderate turbine inlet temperature region and compact footprint due to the small components and simple layout. As shown in Figure 1, S-CO_2 cycle can be coupled to various heat sources [1]. In addition, the S-CO_2 cycle can replace the sodium-water reaction with the mild sodium-CO_2 reaction and improve the reactor safety inherently.

A 75MWe S-CO_2 cycle is designed for the SFR application and the recompression layout is selected. Various Brayton cycle designs for Small and Medium sized SFR application have been investigated and S-CO_2 recompression cycle with radial type turbomachinery has been proven to have still competitiveness [2]. As the target power of the reference SFR is selected to be 150MW, which matches with the current Korean SFR demonstration project, two modules of the S-CO_2 cycle are required. To assess the cycle performance, the corresponding heat exchanger and turbomachinery performances must be found. The turbomachineries and heat exchangers for the 75MWe S-CO_2 cycle are the radial type turbomachinery connected with single shaft and the printed circuit heat exchangers (PCHE). The detailed design process and

results will be discussed in the following sections. The optimized cycle conditions are shown in Figure 2.

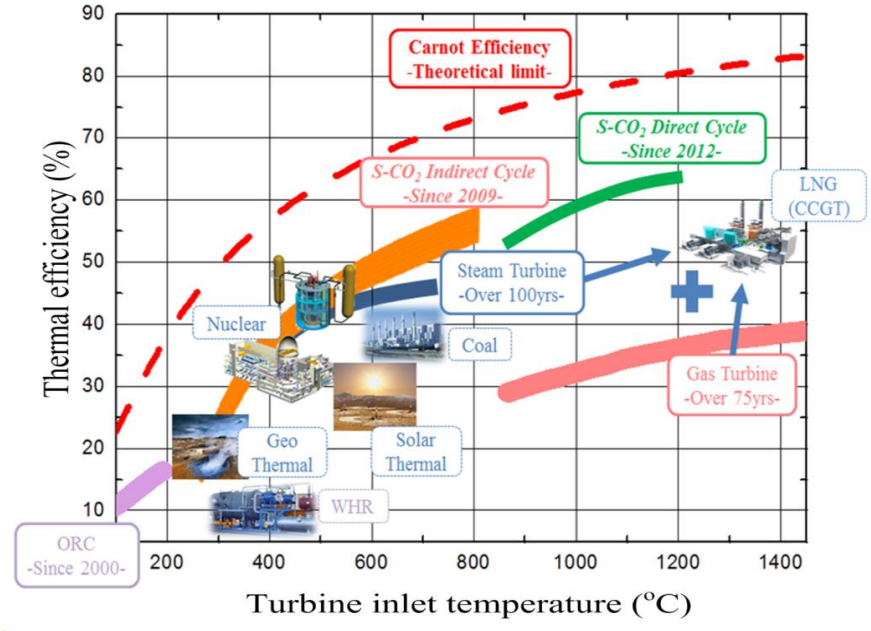

Figure 1. Thermal efficiencies of power conversion systems and applications

* CCGT : Combined cycle gas turbine

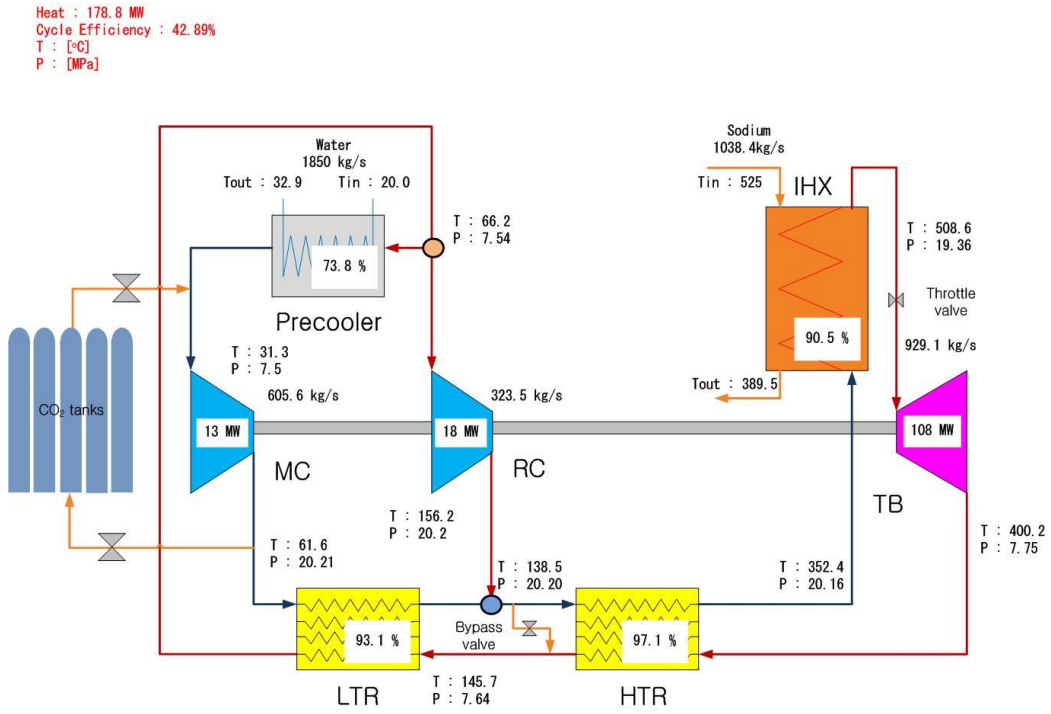

Figure 2. S-CO_2 cycle condition for SFR application

* TB : turbine, MC : main compressor, RC : recompression compressor,

IHX : intermediate heat exchanger, HTR : high temperature recuperator,

LTR : low temperature recuperator

II. S-CO_2 cycle and component design

II.1. Turbomachinery design

As the system power output increases, the related turbomachinery technology becomes different. Generally, in a large scale system, axial type turbomachineries are favored over other types. For example MW scale conventional gas turbines and helium turbine-compressors are usually designed as axial type. However, in the S-CO_2 cycle, radial type turbomachineries can be more appropriate even for the relatively large scale MW output system due to the high density and low pressure ratio cycle characteristics [3].

To design a radial type turbomachinery, the KAIST research team developed an in-house turbomachinery design code (KAIST-TMD) which is an one dimensional mean-line design code. As CO2 thermodynamic properties vary dramatically near the critical point, the conventional design code based on the ideal-gas assumption is not applicable. The NIST (National Institute of Standards and Technology) property database is used, and the continuity equation and Euler turbine equation are directly solved with the real gas property. Various loss models referred from open literatures are used in KAIST-TMD code. The design results from KAIST-TMD are partially verified with the experiment data from SNL [4]. The design results of a 75MWe S-CO_2 cycle are shown in Table 1 and Figures 3-5.

Table 1. Turbomachinery design parameters of 75MWe S-CO_2 cycle

Turbomachinery	Turbine	Main Compressor	Recompression Compressor
Type	Radial		
Stage number	1		
Rotating speed, rpm	7200		
Power, MW	108.2	13.0	18.6
Flow rate, kg/s	929.1	605.6	323.5
Inlet temperature, ^oC	508.6	31.3	66.2
Inlet pressure, MPa	19.36	7.5	7.54
Pressure ratio	2.5	2.69	2.68
Impeller diameter, m	0.95	0.55	0.74
Maximum Mach Number	0.77	0.22	0.30
Total-to-total efficiency, %	92.5	88.2	91.1
Head (Loading) coefficient, m	0.98	0.62	0.67
Flow coefficient	0.023	0.027	0.016

II.2. Heat exchanger design

For the S-CO_2 cycle application, the Printed Circuit type Heat Exchanger (PCHE) has been widely used in the previous works as it can operate under high temperature and high pressure conditions with high compactness. KAIST research team developed an in-house heat exchanger design code (KAIST-HXD) and the algorithm is shown in Figure 6 [5]. The corresponding heat transfer and friction factor correlations are shown in Table 2.

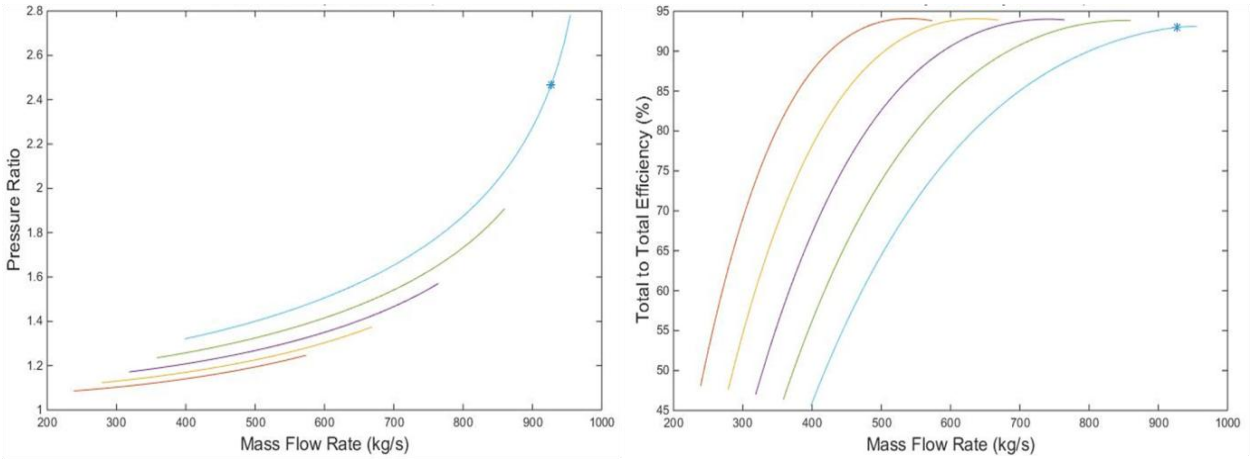

Figure 3. Turbine performance map (Pressure ratio, Total-to-total efficiency)

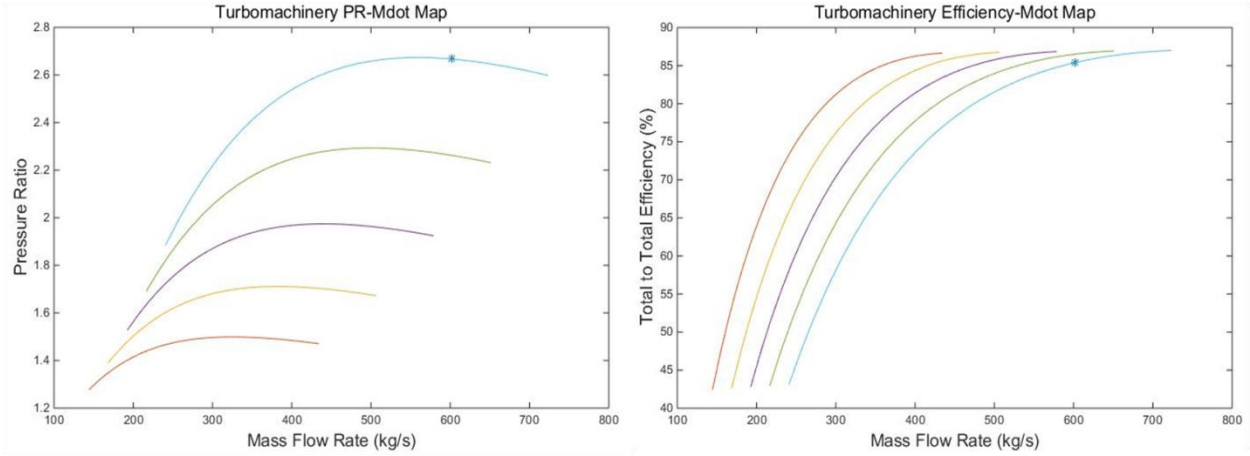

Figure 4. Main compressor performance map (Pressure ratio, Total-to-total efficiency)

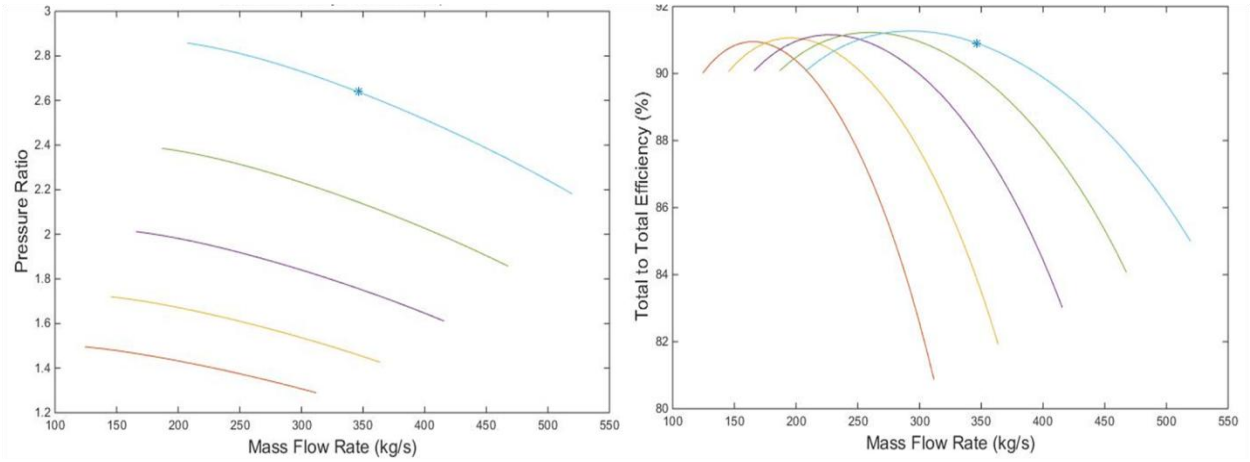

Figure 5. Recompression compressor performance map (Pressure ratio, Total-to-total efficiency)

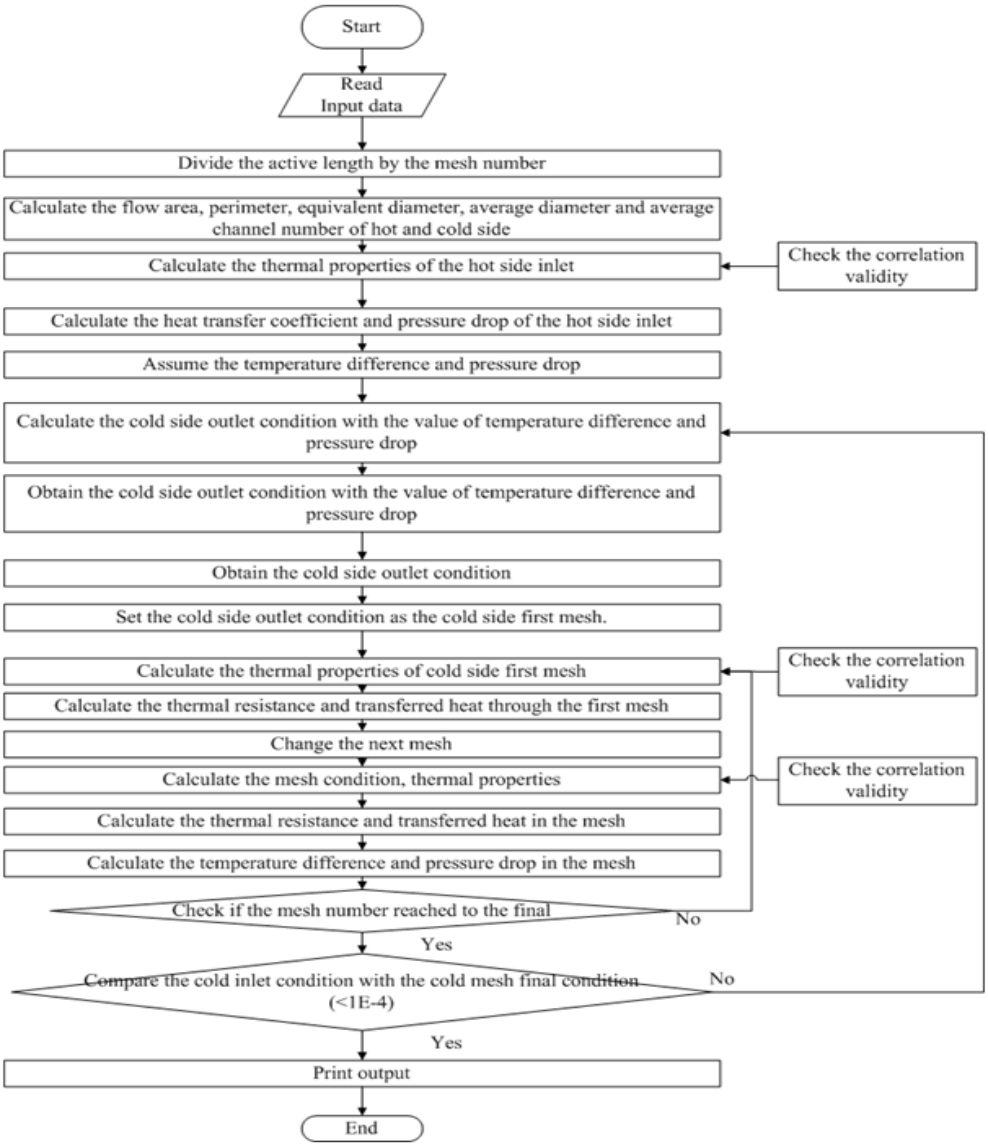

Figure 6. KAIST-HXD algorithm

Table 2. Heat transfer and friction factor correlation in PCHE [4, 5]

Fluid	Na	CO_2	Water
Nusselt number	$\mathrm{Nu} = 7 + 0.025\mathrm{Pe}^{0.8}$	$\mathrm{Nu} = 0.1696\mathrm{Re}^{0.629}\mathrm{Pr}^{0.317}$	
Friction factor	$\mathrm{f} = 4(0.0014 + 0.125\mathrm{Re}^{-0.32})$	$\mathrm{f} = 0.1924\mathrm{Re}^{-0.091}$	
N_{Re} range	No limitation	2,500 - 33,000	
Reference	Hejzlar et al., 2007	Ngo et al., 2007	

The design results are shown in Table 3. When the PCHE is designed as multi-modules, manufacturing process, repairing and maintenance works can be easier. The dimensions of the heat exchanger geometry are limited by the current manufacturing capabilities of the PCHEs manufacturing companies.

Table 3. Heat exchanger design parameters of 75MWe S-CO_2 cycle

Heat exchanger	HTR	LTR	PC	IHX
Heat, MW	108.2	268.7	102.1	178.8
Effectiveness, %	97.1	93.1	73.8	90.5
Volume, m^3	6.9	8.5	3.07	2.3
Geometry, m (L x W x H)	1.1 x 2.5 x 2.5	1.4 x 2.5 x 2.5	1 x 1.75 x 1.75	0.6 x 2.1 x 2.1

II.3. Pipe design

II.3.1 Determination of Pipe Diameter and Thickness of S-CO_2 cycle

When designing a pipe system, energy costs, corrosion, erosion, noise, vibration, system requirement (pump inlet/outlet etc.), pressure loss, and thermal expansion should be typically considered [7].

However, determining the pipe diameter after reviewing all the above-mentioned aspects requires tremendous amount of effort and time. Therefore, to minimize these efforts, most engineering companies establish criteria for the optimal flow velocity as a design guideline. This is shown in Figure 7.

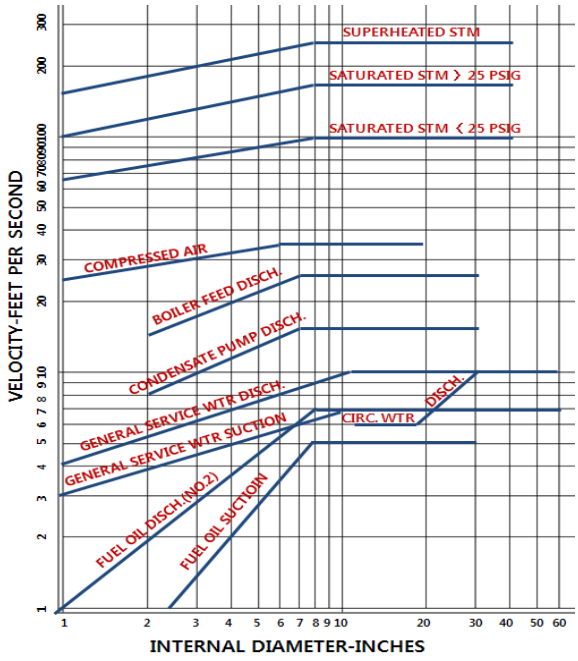

Figure 7. Optimal flow velocities of various piping systems [8]

Although there is an optimal flow velocity in the pipe for water and steam, there was no similar approach for designing the S-CO_2 cycle. Thus, as a preliminary study, the following equation was first applied to define the pipe dimensions for the S-CO_2 cycle. The equation is an empirical formula suggested by Ronald W. Capps for general fluids [9].

$$V = f_{pv}/\rho^{0.3} \quad (1)$$

PIPE VELOCITY FACTORS	
Motive Energy Source	m(kg/m^3)$^{0.3}$/s
Centrifugal pump, Blower	14
Compressor Pipe dia<6in.	24
Pipe dia>6in.	29
Steam Boiler	63~68

V: optimal flow velocity [m/s]
f_{pv}: pipe velocity factor [$m(kg/m^3)^{0.3}/s$]
ρ: density of flow [kg/m^3]

In the case that the diameter of pipe is larger than 6 in., the optimal velocity factor is 29. To determinate the pipe diameter and thickness in accordance with the ASME standard, temperature and pressure should be considered. In addition, as the selection of pipe material affects the minimum thickness and the cost of a pipe, the overall economy of the pipe material selection has to be studied further. The procedure to comply with the ASME standard is as follows:

① After obtaining the average diameter from the optimal velocity, calculate the minimum required thickness. The equation of minimum required wall thickness is as follows:

$$t_m = \frac{PD_o}{2(SE + Py)} + A \tag{2}$$

where t_m is minimum required wall thickness [m], *P* is internal design pressure [Pa], D_o is outside diameter of pipe [m], *S* is maximum allowable stress [Pa], *E* is weld joint efficiency, y is coefficient, and *A* is additional thickness [m].

② Set the outside diameter and thickness in accordance with the ASME standard by selecting the proper material.
③ In the case that the flow velocity is more than the optimal velocity, select larger outside diameter pipe and check whether it complies with the ASME standard.
④ If there is no standard thickness which is suitable for designed diameter or diameter is too large compared to the system, find proper minimum required thickness by reducing the diameter by trading off the system performance with the pressure drop.
⑤ After 1-4 process, re-examine whether the thickness is larger than the revised minimum required thickness.

II.3.2 Pipe Design and Sizing Results

The optimal diameters and thicknesses in accordance with the ASME standard were calculated for the 75MWe S-CO_2 power conversion system. The results are shown in Table 4.

Table 4. The optimal diameter and thickness of 75MWe S-CO_2 cycle in accordance with the ASME standard

Section Condition	Nominal Pipe Size	External Diameter (m)	Velocity (m/s)	Thickness (mm)	Material type	Pressure drop (kPa)
① Turbine Inlet	24	0.610	31.8	0.03493	Nickel and High Nickel Alloys, N06600, B 168	46.68
② HT Recuperator HS Inlet	28	0.711	42.7	0.01905	Nickel and High Nickel Alloys, N06600, B 168	28.47
③ LT Recuperator HS Inlet	28	0.711	25.3	0.01905	Nickel and High Nickel Alloys, N06600, B 168	60.78
④ LT Recuperator HS Outlet	28	0.711	15.8	0.01748	Low and Intermediate Alloy Steel, P91 A335	8.50
⑤ Pre-cooler Inlet	28	0.711	10.3	0.01748	Low and Intermediate Alloy Steel, P91 A335	13.17
⑥ MC Inlet	24	0.610	3.9	0.01588	Low and Intermediate Alloy Steel, P91 A335	0.91
⑦ LT Recuperator CS Inlet	24	0.610	3.7	0.03493	Nickel and High Nickel Alloys, N06600, B 168	2.25
⑧ LT Recuperator CS Outlet	24	0.610	7.7	0.03493	Nickel and High Nickel Alloys, N06600, B 168	22.95
⑨ RC Inlet	24	0.610	7.6	0.01588	Low and Intermediate Alloy Steel, P91 A335	4.75
⑩ RC Outlet	24	0.610	4.4	0.03493	Nickel and High Nickel Alloys, N06600, B 168	2.81
⑪ HT Recuperator CS Inlet	24	0.610	12.5	0.03493	Nickel and High Nickel Alloys, N06600, B 168	6.94
⑫ IHX Inlet	24	0.610	23.8	0.03493	Nickel and High Nickel Alloys, N06600, B 168	89.39
Total pressure drop including minor loss (kPa)						287.60

2.5 mm of additional pipe thickness is added for the safety margin. The used materials are combinations of high nickel alloys 600, which is used in the pressure water reactor (PWR), and low and intermediate alloy steel. All the figures of S, E, y are found in the ASME B31.1 [10]. To minimize the pressure drop and footprint, an optimal arrangement of components and pipes was found. The length of the highest pressure drop sections (①, ②, ③, and ⑫) are reduced as much as possible. The pressure drop in each path is calculated by using the next expression.

$$\Delta p = f \cdot \frac{L}{D} \cdot \frac{\rho V^2}{2} \tag{3}$$

where Δp is pressure drop [Pa], f is friction factor, L is length of pipe [m], D is internal diameter of pipe [m], ρ is density of flow [kg/m^3], and V is optimal flow velocity [m/s].

Friction factor is calculated by a Colebrook equation which is a function of Reynolds number and surface roughness:

$$\frac{1}{\sqrt{f}} = -1.8 \log[(\frac{\varepsilon / D}{3.7})^{1.11} + \frac{6.9}{Re}] \quad (4)$$

where f is friction factor, ε is roughness, D is internal diameter of pipe [m], and R_e is Reynolds number of pipe.

Also, it was considered that there are three 90° bends in ③, ⑤, and ⑫ section, two 90° bends in ①, and ⑧ sections, and one 90° bend in ②, ④, ⑨, and ⑩ sections. Moreover, the minor losses should be considered. The minor losses in each path are calculated using the expression.

$$\Delta p = K_L \cdot \frac{L}{D} \cdot \frac{\rho V^2}{2} \quad (5)$$

where K_L is loss coefficient

Each K_L value is 0.3 at 90° bend, 0.2 at 45° bend, 0.26 at T-shape pipe for flow split, and 0.2 at mixing T-shape pipe, respectively [11]. The total pipe pressure drop compared to the overall system pressure is 1.42 %.
After considering the pressure drop from the pipe system, the cycle thermal efficiency drops by 0.74 %. Although the total pipe pressure drop is somewhat high since the S-CO_2 cycle has high pressure and temperature operating conditions and requires high mass flow rate, the cycle thermal efficiency is still higher than the existing steam Rankine cycle. The final pipe design of the S-CO_2 Recompression cycle applying ball joints is shown in Figure 8. The total volume is approximately 9.7 m × 7.6 m × 2.9 m and the total mass is approximately 3990.2 kg. It is noted that the working fluid mass in the pipes and heat exchangers was considered and in the internal turbo-machinery was neglected as it is relatively negligible compared to the total mass.

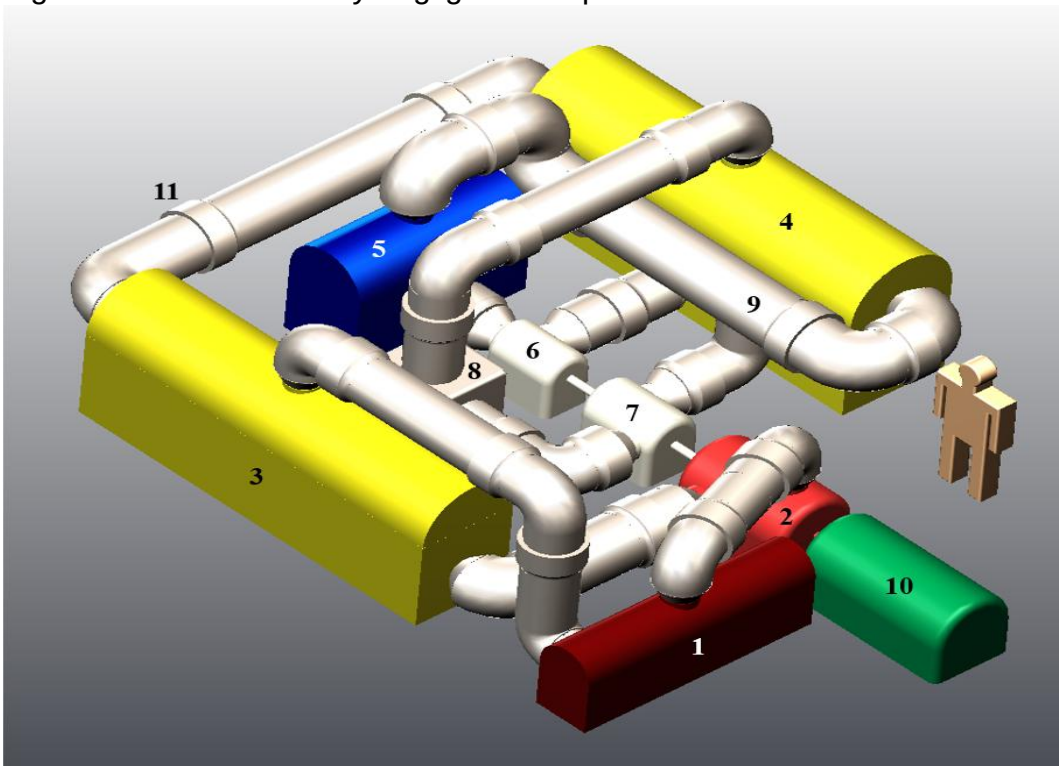

Figure 8. Conceptual pipe design of S-CO_2 Recompression cycle

II.4. Recovery system design

For the CO_2 recovery system design, calculating the leak rate in turbo-machinery is essential to estimate how CO_2 inventory recovery system affects cycle thermal efficiency. To perform the preliminary design, conventional leak rate is assumed, which the conventional leak rate is less than 1kg/s per seal. The labyrinth seal type was preferentially selected because it is easier to analyze the internal flow due to the geometry simplicity and it is more economically feasible than dry gas seal type.

Firstly, the inventory recovery system which discharges the leakage to ambient and refills the CO_2 from a gas tank was considered. However, another recovery method was considered to reduce the thermal efficiency losses due to the CO_2 recovery process since the inventory recovery system which discharges the CO_2 leakage to ambient and refills the CO_2 from the gas tank had relatively high thermal efficiency losses. Figure 9 shows a schematic of the preliminary CO_2 inventory recovery system design of the S-CO_2 power cycle for 75MWe SFR application.

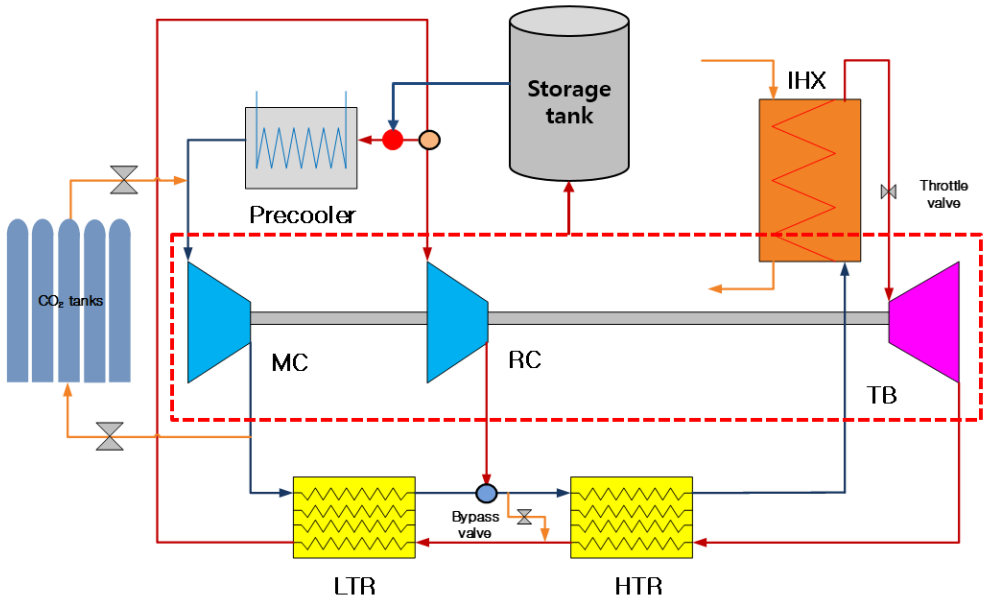

Figure 9. Preliminary design on CO_2 inventory recovery system of S-CO_2 power cycle for 75MWe SFR application

The conditions of storage tank is set as 66.2 ºC and 7.6 MPa. 66.2 ºC is the same with the temperature of the pre-cooler inlet but 7.6 MPa is a bit higher than 7.54 MPa which is the same with the pressure of the pre-cooler inlet to prevent the back flow. By directly connecting rotor cavity to the storage tank, leakage flow goes to the storage tank. However, it was assumed that there is no pressure loss and heat loss in the connecting pipes from rotor cavity to the storage tank. Additionally, it was assumed that additional work to maintain the conditions (66.2 ºC and 7.6 MPa) is negligible. The suggested concept does not require additional compressor to compress liquid CO_2 from the CO_2 tank. The $W_{net,loss}$ of new simple inventory recovery system was calculated through the following equation.

$$W_{net,loss} = W_{net,design} - W_{net,new} \quad (6)$$

$$= W_{net,design} - \left(W_{turb,new} - W_{comp,new}\right)$$

$W_{net,new}$ means the changed net work due to the $\dot{m}$ change of turbines and compressors by considering the seals. By adopting the newly proposed simple method, $W_{net,loss}$ is estimated to be 0.312 MW_e. It means that the thermal efficiency losse caused by CO_2 inventory recovery system may become 0.17 % when the conventional leak rate is assumed. The calculation results are summarized in Table 5.1. Therefore, this shows that developing a good seal technology for the S-CO_2 power system operating conditions are very important for the overall system performance.

Table 5. Calculation results of the leak rate in turbo-machinery (No. of seal: 3) [upper], and loss calculation result of net work and thermal efficiency [lower]

Storage tank (Low-pressure tank)	Leakage position (High-pressure tank)	T (℃)	P (MPa)	$\dot{m}$ (kg/s)
66.2 ℃ 7.6 MPa	1. TB inlet	508.6	19.36	1.0
	2. MC outlet	61.6	20.21	
	3. RC outlet	156.2	20.20	
Total mass flow rate				3.0

N of Seal point	$W_{net,loss}$ (MW_e)	$\eta_{net,loss}$ (%)
3	0.312	0.17

III. Part load operation control strategy of S-CO_2 cycle

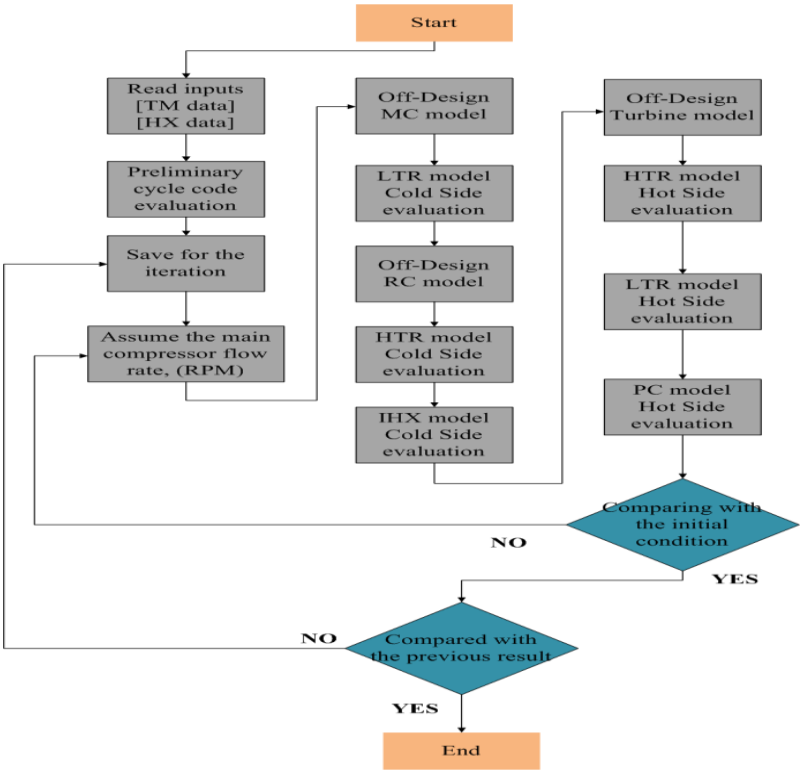

Figure 10. S-CO_2 cycle quasi-static analysis code algorithm

To establish the control logic for the part-load operation, an in-house quasi-static cycle analysis code was developed by KAIST research team. The quasi-static analysis code algorithm is shown in Figure 10. The heat exchanger and the turbomachinery geometries are used from the component design results.

When the SFR power decreases, the sodium mass flow rate is assumed to linearly decrease while the temperature gradient in the intermediate heat exchanger is maintained. For the part-load operation, three control logics (inventory, turbine throttle and bypass valve control) are assumed as shown in Figure 2. As shown in Figure 11, the inventory control is the most efficient control mechanism for the part load operation. However, the inventory control generally lacks of rapid response, and thus the valve controls must be adopted to deal with the fast transient cases. The valve control is relatively less efficient with respect to the part load cycle thermal efficiency.

During part load operation, the operating condition of turbomachinery varies as well. Therefore, the equivalent mass flow rate is used to consider the discrepancy between the operating and design condition when the turbomachinery performance map is applied. The turbomachinery works and main compressor inlet conditions under part load condition are assessed as shown in Figures 12 and 13. The turbine work is significantly decreased compared to the compressor works under the part load condition. The compressor surge is the condition at which the compressor is not capable of providing enough energy to overcome the system resistance or backpressure. Therefore, the compressor surge condition must be avoided in any cases during the system operation. As shown in Figures 12 and 13, the main compressor surge margin rapidly decreases under the part load operating conditions. Therefore, the valve control must be applied during the low load operation.

$$\dot{m}_{eq} = \dot{m}\frac{\sqrt{\theta}}{\delta}\varepsilon \tag{7}$$

$$\theta = \left[\frac{\frac{\gamma_a}{\gamma_a + 1}T_a}{\frac{\gamma_{ref}}{\gamma_{ref} + 1}T_{ref}}\right]^2 \tag{8}$$

$$\delta = \frac{P_a}{P_{ref}} \tag{9}$$

$$\varepsilon = \frac{\gamma_{ref}\left(\frac{2}{\gamma_{ref} + 1}\right)^{\frac{\gamma_{ref}}{\gamma_{ref} - 1}}}{\gamma_a\left(\frac{2}{\gamma_a + 1}\right)^{\frac{\gamma_a}{\gamma_a - 1}}} \tag{10}$$

where $\dot{m}$, γ, P, T are mass flow rate, specific heat ratio, pressure and temperature, respectively.

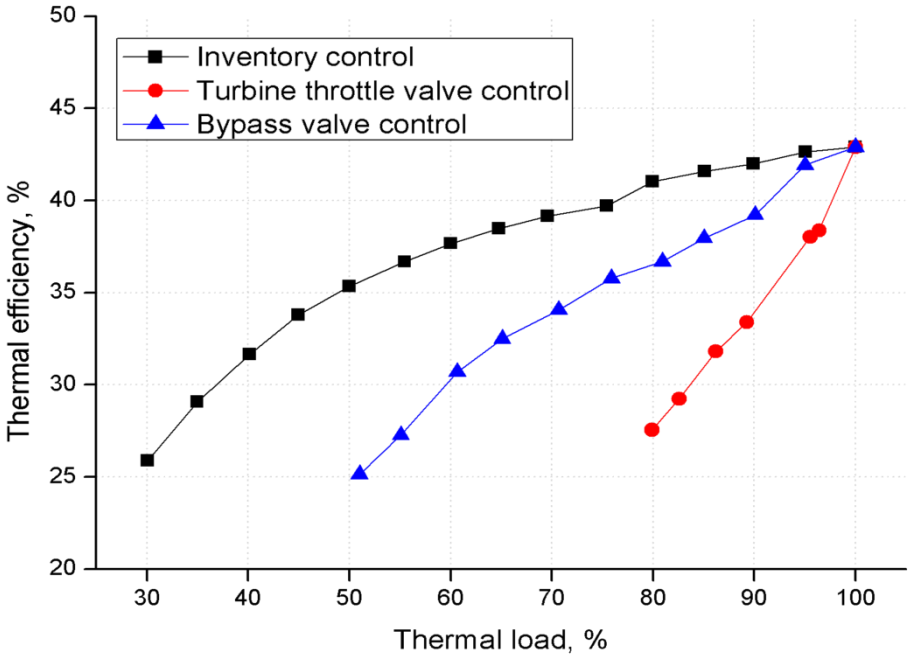

Figure 11. Comparison of S-CO_2 cycle performance in part load conditions

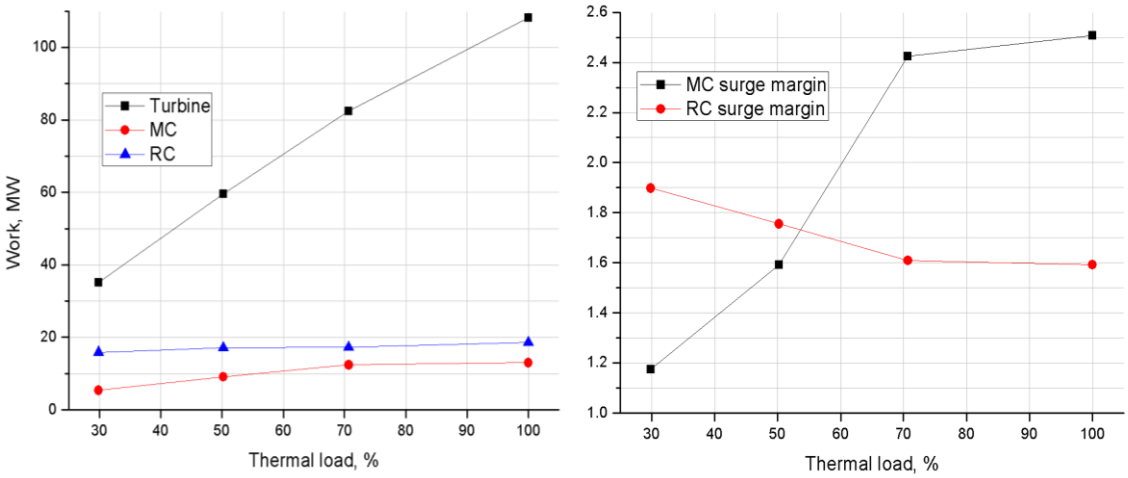

Figure 12. Comparison of turbomachinery works and compressor surge margin in part load conditions

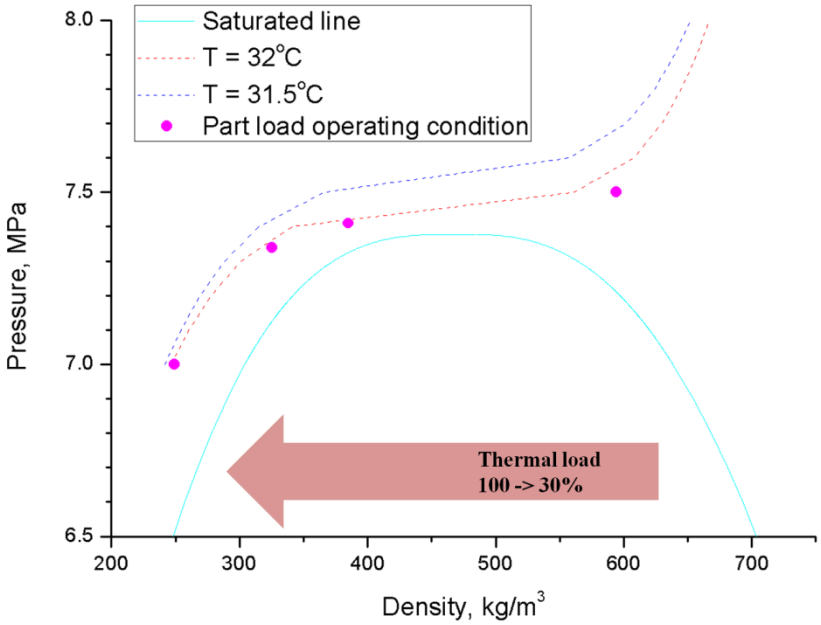

Figure 13. Part load main compressor inlet condition

IV. Summary and future work

A 75MWe S-CO_2 recompression cycle with radial type turbomachineries and PCHE was designed by combining multiple design codes developed in-house. Based on the component design parameters, the pipe system and the concept of overall system module were described. Furthermore, by considering the leakage flow from turbomachineries, adequate recovery tank volume was calculated. The leakage flow and physical phenomena in the turbomachinery seal sections will be further studied in the future. To establish the control strategies under part load operation, an in-house quasi-static cycle analysis code was developed and three control logics including inventory, turbine bypass and throttle valve controls are assessed for the part load cycle performance. The inventory control is the most efficient control mechanism for the part load operation but the compressor surge margin of the main compressor decreases rapidly for the lower (<50%) part load condition. To establish the most efficient strategy for the part load conditions, the potential of the valve and inventory controls will be further investigated.

V. Acknowledgement

This work was supported by the On Demand Development Program of Core Technology for Industrial Fields (10054621, Development of a FEED Framework for Next Generation Power System using Pilot Plant) funded By the Ministry of Trade, industry & Energy (MI, Korea)

VI. Nomenclature

S-CO_2: Supercritical carbon dioxide

SFR: Sodium-cooled fast reactor

PCHE: Printed circuit heat exchangers

CCGT : Combined cycle gas turbine

TB : Turbine

MC : Main compressor

RC : Recompression compressor

IHX : Intermediate heat exchanger

HTR : High temperature recuperator

LTR : Low temperature recuperator

KAIST-TMD: Korea advanced institute of science and technology- turbomachinery design code

NIST: National institute of standards and technology

KAIST-HXD: Korea advanced institute of science and technology- heat exchanger design code

V: Optimal flow velocity [m/s]

f_{pv}: Pipe velocity factor $[\mathrm{m(kg/m^3)^{0.3}/s}]$

ρ: Density of flow $[\mathrm{kg/m^3}]$

ASME: American society of mechanical engineer

t_m: Minimum required wall thickness [m]

P: Internal design pressure [Pa]

D_o: Outside diameter of pipe [m]

S: Maximum allowable stress [Pa]

E: Weld joint efficiency

Y: Coefficient

A: Additional thickness [m]

NPS: Nominal pipe size

$\Delta\mathrm{P}$: Pressure drop [Pa]

f: friction factor

L: length of pipe [m]

D: Internal diameter of pipe [m]

ε: Roughness

Re: Reynolds number of pipe

K_L: Loss coefficient

VII. Reference

[1] Y. Ahn, S. J. Bae, M. Kim, S. K. Cho, S. Baik, J. E. Cha, 2015, "REVIEW OF SUPERCRITICAL CO2 POWER CYCLE TECHNOLOGY AND CURRENT SATUS OF RESEARCH AND DEVELOPMENT", Nucl. Eng. Technol, 47(2015) 647-661

[2] Y. Ahn, J. I. Lee, 2014, "Study of various Brayton cycle designs for small modular sodium-cooled fast reactor", Nucl. Eng. Des, 276(2015) 128-141

[3] J. J. Sienicki, A. Moisseytsev, R. L. Fuller, S. A. Wright, P. S. Pickard, 2011, "Scale Dependencies of Supercritical Carbon Dioxide Brayton Cycle Technologies and the Optimal Size for a Next-Step Supercritical CO2 Cycle Demonstration", SCO2 Power Cycle Symposium, May 24-25, 2011, Boulder, Colorado

[4] J. Lee, J. I. Lee, H. J. Yoon, J. E. Cha, 2014, "Supercritical Carbon Dioxide turbomachinery design for water-cooled Small Modular Reactor application", Nuclear Engineering and Design, 270(2017), 76-89

[5] P. Hejzlar, M. J. Driscoll, Y. Gong, S. P. Kato, 2007, "Supercritical CO2 Brayton cycle for medium power applications", Final report, MIT-ANP-PR-117

[6] T. L. Ngo, Y. Kato, K. Nikitin, T. Ishizuka, 2007, "Heat transfer and pressure drop correlations of microchannel heat exchangers with S-shaped and zigzag fins for carbon dioxide cycles", Experimental Thermal Fluid Science, 32(2007), 560-570

[7] H. W. Jin, Selection Process of Pipe Diameter and Thickness and Role of Piping Specification when Piping Design, Research Paper of KEPCO Engineering & Construction (2010).

[8] Pipe Velocity Guideline (DS-M-1201), KEPCO-ENC.

[9] Ronald W. Capps, Fluid Handling, textbook of the Gulf Coast Consulting Group (2013).

[10] ASME B31.1(Power Piping), ASME (2010).

[11] Li Xin, Wang Shaoping, Flow field and pressure loss analysis of junction and its structure optimization of aircraft hydraulic pipe system, Chinese Journal of Aeronautics (2013).